Supernova Neutrinos in XENONnT GDR Duphy Aussois

Layos Daniel Garcia
layos.daniel@lpnhe.in2p3.fr

PhD Student

June 22, 2023

LPNHE

3 Sensitive SNν Detection Volumes :
TPC with 5.9 T LXe
n and μVetos with total **700 T Water**

Core Collape Supernova CCSN

~3x10e53 ergs ν emission

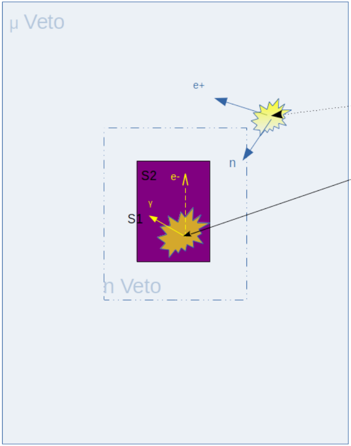

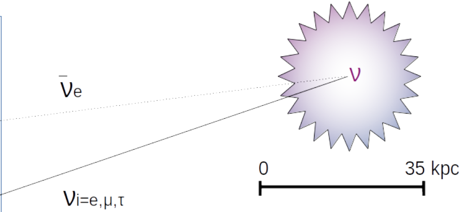

Neutrino -Xe Coherent Scatttering CνNS
Sensible to all ν flavours (**90–190 evts.** at 10 kpc)

ν + Xe ⟶ ν + *Xe (Scintillation S1, S2)

Inverse Beta Decay IBD (70–175 evts. at 10 kpc**)**

ν_e + p ⟶ e^+ + n (**Cerenkov light**)

Core collapse Supernova CCSN

- CCSN Spectroscopic classification: **Types II (H-line), Types Ib(He-line), Ic(No He-line)**
- CCSN Progenitors: Massive Stars **8 - 50** $M_\odot$ gravitational core collapse
- Neutrino emission is the energy loss mechanism (99%) for CCSN [1]:

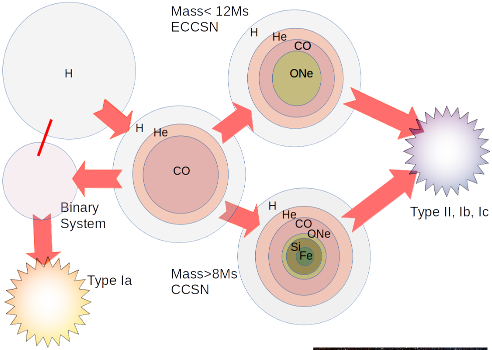

$$\Delta(E_G.) \simeq \left(\frac{3G_N M^2}{5R}\right)_{core} \simeq 3 \times 10^{53} \text{ erg}\,, \qquad (1)$$

- $\sim$**10-15** MeV neutrino burst of all flavours
- $\sim$ **10 -20 s** after bounce of the core
- Neutrino burst detected from SN 1987A 20 events (Kamiokande-II and IMB) [2]

Figure 1: SN 1987 A

Supernova Neutrinos Flux at the earth

$N_{\nu_e} > N_{\bar{\nu}_e} > N_{\nu_x}$ with $x = \mu, \bar{\mu}, \tau, \bar{\tau}$[3]

Neutrino Flux $$\frac{dN}{dEdt}_i = \frac{1}{4\pi d^2} \frac{L_\nu(t)_i}{< E_\nu(t)_i >} \Phi_i(E,t)\psi_i(t) \quad (2)$$

Neutrino energy distribution $$\Phi_i(E,t) = \frac{E^{\alpha(t)_i}}{< E_\nu(t)_i >^{\alpha(t)_i}} e^{-(\alpha(t)_i+1)\frac{E_\nu}{<E_\nu(t)_i>}} \quad (3)$$

Normalisation $$\psi_i(t) = \frac{1}{\int \Phi_i(E,t)dE} \quad (5)$$

- **d distance** of Supernovae
- **Luminosity** $L_{\nu_\beta}(t_{\mathrm{pb}})$
- **Neutrino mean energy** $\langle E_{\nu_\beta}(t_{\mathrm{pb}})\rangle$
- **pinching parameter** $\alpha(t_{\mathrm{pb}})$:

$$\alpha = \frac{\langle E_\nu^2(t_{\mathrm{pb}})\rangle - 2\langle E_\nu(t_{\mathrm{pb}})\rangle^2}{\langle E_\nu(t_{\mathrm{pb}})\rangle^2 - \langle E_\nu^2(t_{\mathrm{pb}})\rangle} \quad (4)$$

Transport effects:

- Matter effects MSW [4]
- Flavor Oscillations

A lot of CCSN models since SN1987A...
SNEWPY [5]

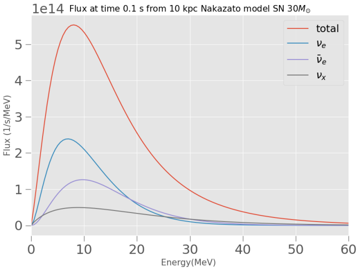

Figure 2: differential flux from Nakzato simulation Model with a progenitor mass of 30 $M_\odot$ at a time of 0.1s after the bounce

SNEWS SuperNova Early Warning System [6]

Several detector network advantages

- Multiple Detector coincidences
- Directionnal information
- Time signal reconstruction

Requirements

- Reduction of Non-poisonian background
- High false alert rejection
- GPS synchro-data

Communication

- Alerts
- Mail list
    - Astronomical community & amateur astronomers
    - SN neutrino* experiments

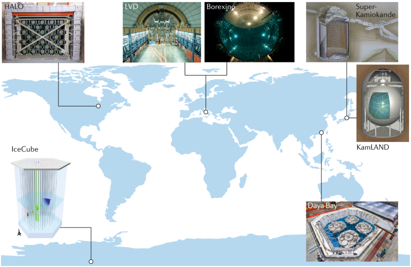

Neutrino detectors:

Super-Kamiokande, IceCube, KM3NeT, KamLAND, SNO+,NOvA, HALO

Gravitational waves detectors: alerts from LIGO and Virgo

and Dark Matter detectors... XENONnT soon!

XENON Working group SNMultimessenger

Done (green) | Current (orange)

Type of analysis	Task
Communication	GPS timestamps
	Communication scheme
	Alarm procedure
	DAQ integration
	Comm Testing
Simulations	SNv in TPC wfsim
	Sims varying with SN distance
	SNv in geant4 sims (Done)
	MV & NV sims in wfsim (Current)
Cuts	Peak level cuts
	Time window cuts
	Cut optimization check with SN distance
	MV & NV background study (Current)
Trigger	Define thresholds
	Inject sim into background run
Sensitivity	Sensitivities as a function of distance
	Charge current interactions
	False alarm rate
	Light curve reconstruction
MMA	Fire drills with SNEWS
	Connect with LIGO server and stay active with TPC

SNEWS

- Time GPS
- online DAQ
- Trigger Alarms
- Comunication
  - Test alarms
  - Mail lists

CCSN ν signal

- TPC (S2 only)
  - CSNνNS simulation
  - Sensitivities as a function of distance
- Vetos
  - IBD GEANT 4 Simulation
  - Digitalization & Background item
    Include Veto in SNEWS?
- Time reconstruction of SN signal
- SNEWS requierements:
  - False alarms rates
  - Background rates

XENONnT: Direct Dark matter research Experiment

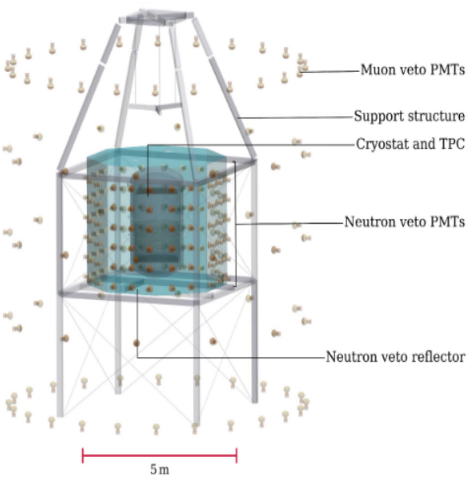

XENONnT TPC is surrounded by **700 T** of pure **Water** :

- **μVeto** (update of **XENON1T**)
  for muons surviving ~1.5km LGNS rock <Eμ>~270 GeV

- **nVeto** (update in **XENONnT**) :
  radiogenic neutrons from detector materials

WIMP* – *Xe nuclear (e) recoil :

Dual Phase Time Chamber TPC **(5.9 T Xe)**

S1 (prompt) scintillation
S2 (proportional) from Ionization

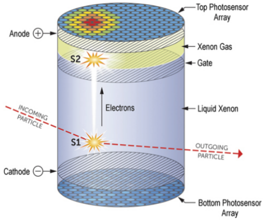

Ratio (S2/S1) allows NR and ER discrimination

Sensible to low Recoils ~1 keV(S2 Only)

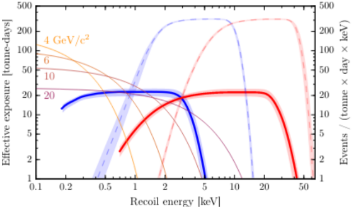

XENONnT TPC CCSN Neutrino Interactions

NC All flavors i= $e, \bar{e}, x, \bar{x}$:

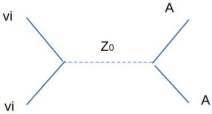

- CEνNS
  - $\nu_i + Xe \rightarrow \nu_i + Xe^*$
  - $\sigma \propto A^2$
  - CCSNν low recoils (0-5 KeV)

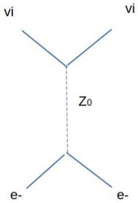

- Electron Scattering ES: $\nu_i + e^- \rightarrow \nu_i + e^-$
  - Directional information
  - Low interaction rate for XENONnT

CC e ($\bar{e}$) flavor

- ES : $\nu_e(\bar{\nu}_e) + e^- \rightarrow \nu_e(\bar{\nu}_e) + e^-$
  - $\approx$ 1/3 of the total SN neutrino flux
- Inelastic Scattering IE: $\nu_e +^{132}$ Xe $\rightarrow e^- +^{132} Cs^*$ [7]
  - Only sensible to ν_e
  - 1.1 MeV γ and neutron emission in a 0.9 fraction
  - Large S2 signal

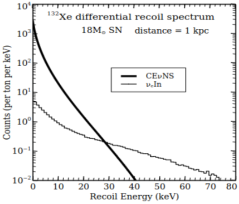

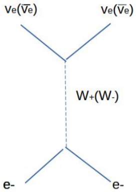

CCSN CEνNS rate in XENONnT TPC

CEνNS Energy recoil E_R differential rate[3]

$$\frac{dN}{dtdE_R} = N_{Xe}\frac{1}{4\pi d^2}\int_{E_{min}}\frac{dN}{dE_\nu dt}\frac{d\sigma(E,E_R)}{dE_R}dE \qquad (6)$$

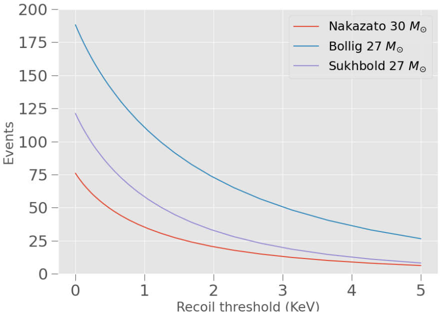

Figure 3: Events for a given threshold at 10 kpc Nakazato 30 $M_\odot$, Sukhbold and Bollig 27 $M_\odot$

- Signal / Bakcground discrimination using SNν high frequency instead of S2/S1 ratio
- **S2 Only**(0.7 KeV)

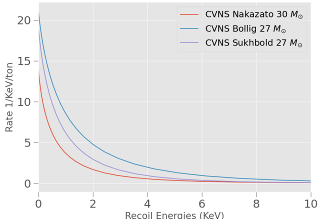

Figure 4: Energy Recoil Rates at 10 kpc Nakazato 30 $M_\odot$, Sukhbold and Bollig 27 $M_\odot$

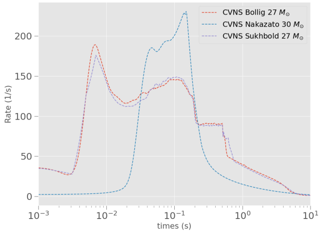

Figure 5: Time Rates at 10 kpc Nakazato 30 $M_\odot$, Sukhbold and Bollig 27 $M_\odot$

CCSN Neutrino Interaction in XENONnT Water Tank

Electron scattering

$\nu_{e,x} + e^- \rightarrow \nu_{e,x} + e^-$

All flavors $\longrightarrow \leq$ 10 events at 10 kpc
Directional information from NC channel
No CC channels for x flavors

Inverse beta decay IBD:

$\bar{\nu}_e + p \rightarrow e^+ + n$

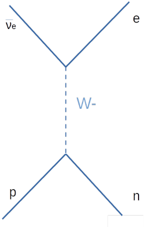

100-200 events at 10 kpc
e+ allow reconstruction of $\bar{\nu}_e$ spectrum
No directional information **e+ emission isotropic**

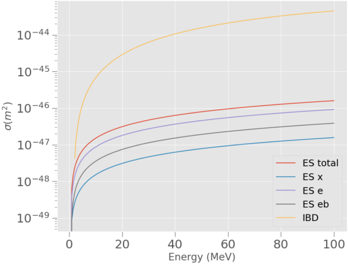

Figure 6: Cross section of neutrino proces in Water tank

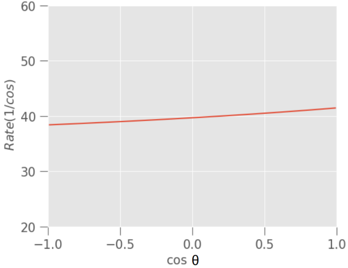

Figure 7: Cosinus of Scattering angle $\bar{\nu}_e$ — $e+$ distribution for Nakazato model

CCSN IBD Spectrums

$E_{\nu_{th}} = 1.806 \text{ MeV} \ll \langle E_\nu \rangle$

e+ Cherenkov threshold $E_{ech_{th}} = 774KeV \rightarrow \beta = \frac{1}{n_w}$ $\quad n_w$=1.33

$E_{\nu ch_{th}} \approx 2.06MeV$

$$\frac{dN}{dtdE} = f_p N_{H_2O} \frac{1}{4\pi d^2} \frac{L(t)}{< E > (t)} \phi(E,t)\psi(t)\sigma(E) \qquad \sigma(E) = \int_{E_{e_1}}^{E_{e_2}} \frac{d\sigma(E, E_e)}{dE_e} dE_e \qquad (7)$$

$$E_{1,2} = E_\nu - \delta - \frac{1}{m_p} E_\nu^{CM} (E_e^{CM} p_e^{CM}), \qquad \delta \equiv \frac{m_n^2 - m_p^2 - m_e^2}{2m_p} \qquad f_p = 2 \qquad (8)$$

$N_{H_2O} \approx 3.32710^{28}$

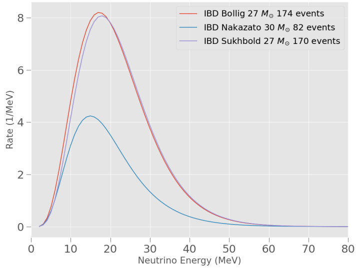

Figure 8: IBD Energy spectrum rates at 10 kpc

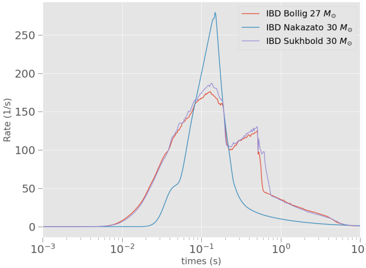

Figure 9: IBD Time spectrum rates at 10 kpc

CEνNS vs IBD rates

- High rates in a 10s window in TPC/Veto
- Total IBD and CνNS rates are similar $V_{veto} \approx 100 V_{TPC}$
- Different time evolution : CνNS (ν_e peak around 10ms) vs IBD ($\bar{\nu}_e$ peak around 100ms)

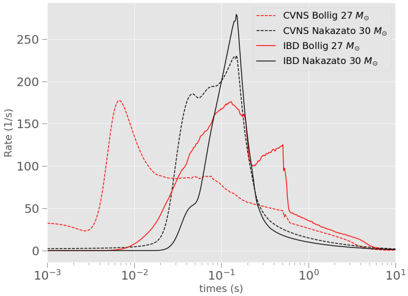

Figure 10: CEνNS vs IBD Time Spectrum Rate for Nakazato and Bollig models at 10 kpc

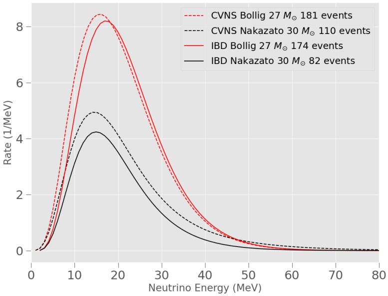

Figure 11: CEνNS vs IBD Energy Spectrum Rate for Nakazato and Bollig models at 10 kpc

- IBD interaction is **homogenously** distributed in Water tank
- e+ emission is **isotropic**
- n, e+ in the **same vertex** or n and e+ **alone** simulation
- **Water** or **Gd** (0.2%) Water configurations

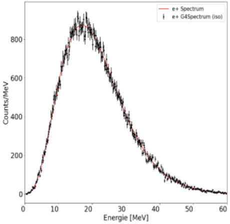

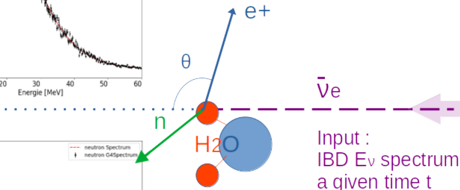

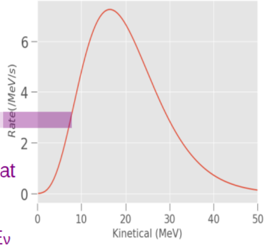

Input :
IBD Eν spectrum at a given time t
or
Mono-energetic Eν

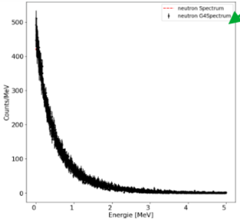

Charge depositions in Water from n and e+
Opticals parameters for Cerenkov light

Neutron and Muon Veto **PMThits**
(ID, Energy, time)

IBD Cerenkov light

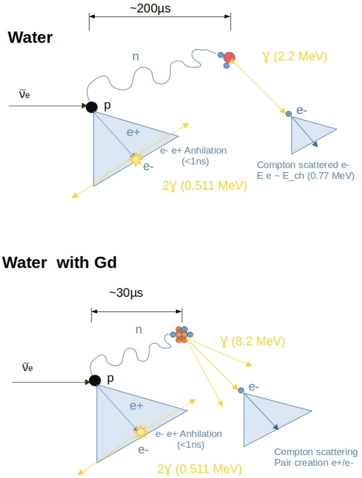

In **Water** most of Cerenkov light is produced by e+, 2.2 MeV γ from nCapture produced compton scattered e- close to the E_{ch}.
In **Water with Gd** More Cerenkov light from 8.2 MeV γ-cascade neutron Gd capture, due to the contribution of e-/e+ .

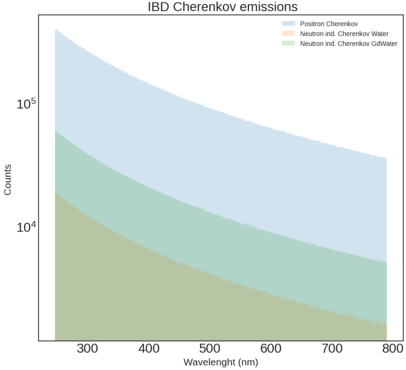

Figure 12: Cerenkov emission in Water vs Gd Water. Positron (blue), neutron GdWater (Green) and neutron Water (orange)

IBD Event time distributions

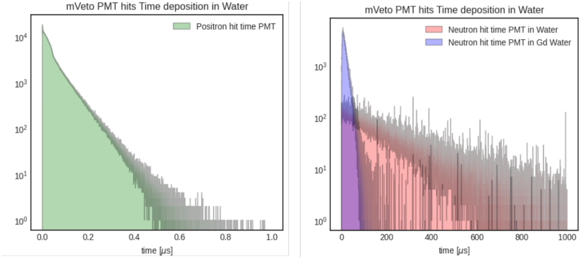

Figure 13: Muon Veto PMT hits depositions

e+ event $\mathcal{O}$ 10 (ns)
n event 0-1 ms (Water) and 0-100 μs (Gd).

Pile up for neutron (in Water) and next positron event.

Pmt hit Time cut

f_{max} $\mathcal{O}(10^2 Hz)$.
$\tau_{cut} = 1ms$

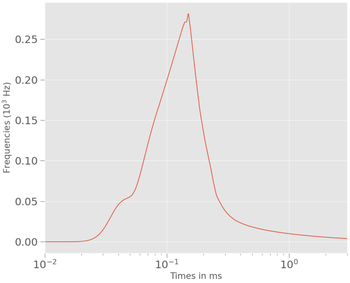

Figure 14: IBD Rates for SN from Nazato model $30M_{\odot}$ around the $\bar{\nu}_e$ peak 0.05-0.20 s

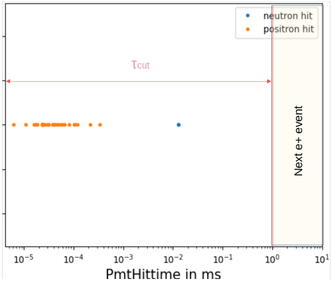

Figure 15: n and e+ hits for an IBD event

nVeto vs Muon Veto

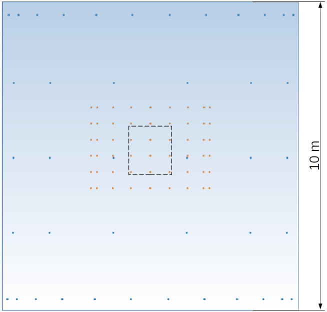

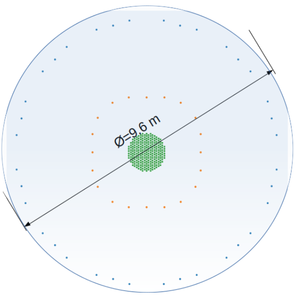

Neutron Veto

120 PMTs (Hammatsu R5912)
V_w~**55m³**
5-12 IBD Events

Muon Veto

84 PMTs (Hammatsu R5912ASSY)
V_w **~645 m³**
80-150 IBD Events

$M_{Vol} / N_{Vol} \sim 11$
$M_{cov} / N_{cov} \sim 0.06$

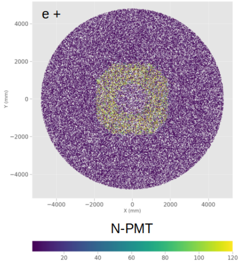

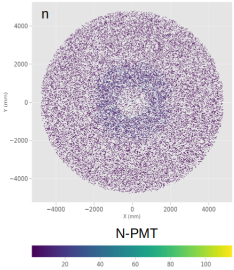

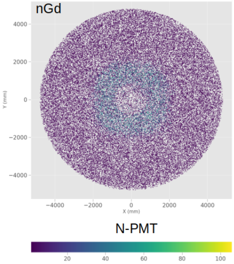

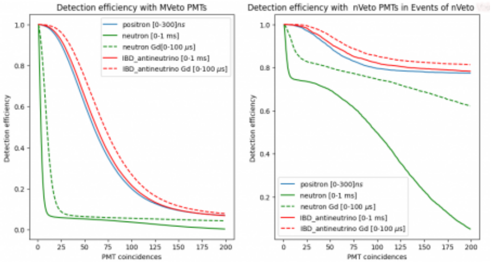

Figure 16: Efficiencies for nVeto(right) and μVeto (left) as a function of PMT coincidences

- GEANT4 **PMThits** digitalization:
    - Detection efficiencies:
        - PMT coincidences
        - e+ Energie
- Background analysis for μ and neutron Vetos
- Reconstruction SN neutrino signal in time:
    - PMTs response as a function of e+ Energy
- Sensitivity Study
- Inclusion of Vetos in SNEWS... **Veto Trigger**

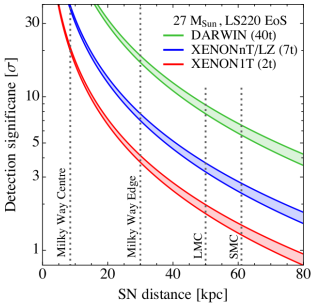

Figure 17: Detection signifiance as a function of SN distance

CEνNS Events (**5σ / SN 27$M_\odot$** (S2 Only, E_{th}=0.7 KeV))[3]

XENON1T	XENONnT	DARWIN
25 kpc 35 events	35 kpc 123 events	65 kpc 704 events

THANK YOU !!!

Remerciements: Elisa Radjabou *Internship M1 PFA - Sorbonne Université*

BACKUP

Neutrino burst from CCSN

- **Collapse and Bounce 0-0.1s** $\mathcal{O}(10^{53} ergs)$

  $p + e^- \longrightarrow \nu_e + n$

  Increase of e- pressure reduced, collapse accelerates
  Core bounce

- **Accretion 0.1-1s** $\mathcal{O}(10^{53} ergs)$

  Density increases and shock wave out of the core

  $e^- + e^+ \rightarrow \nu_e + \bar{\nu}_e$
  $\nu_e + \bar{\nu}_e \rightarrow \nu_{\mu,\tau} + \bar{\nu}_{\mu,\tau}$
  N+N $\rightarrow$ N+N + $\nu\bar{\nu}$

- **Cooling 1-10s** $\mathcal{O}(10^{53} ergs)$

  Luminosity decreases Charge current interactions are supressed
  Proto-neutron Star PNS

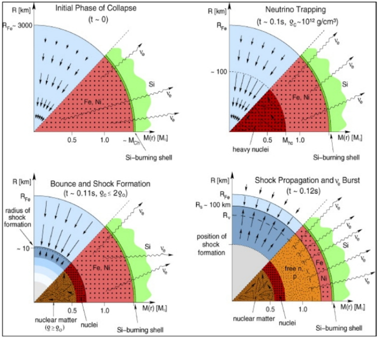

Shock revive mechanism ?

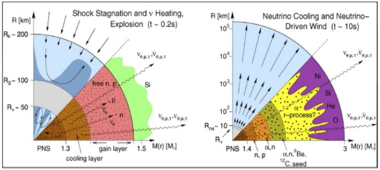

Figure 18: Schema of core collapse[8]

Light Curves & Emission time evolution

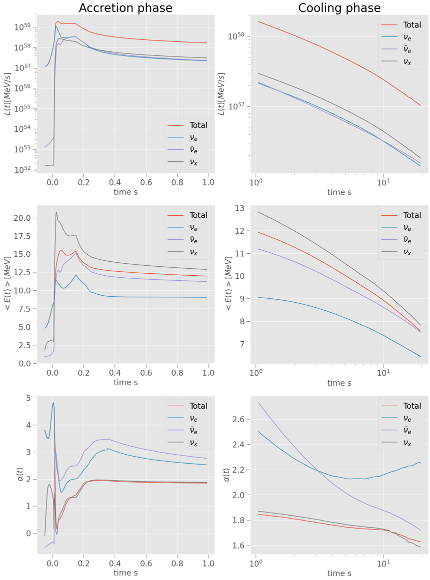

Figure 19: Light curves from Nakazato 30 $M_\odot$

2 Different phases after bounce:

Accretion [0, 1 s]:

- 0 - 0.05 s: ν_e
- 0.05 - 1 s: $\bar{\nu}_e$, ν_x

Cooling phase [1,10 s]

$\langle E_{\nu_e} \rangle \approx 12 MeV$

$\langle E_{\bar{\nu}_e} \rangle \approx 14 MeV$

$\langle E_{\nu_x} \rangle \approx$ 15 MeV

$\langle \alpha \rangle$ [2, 3.5]

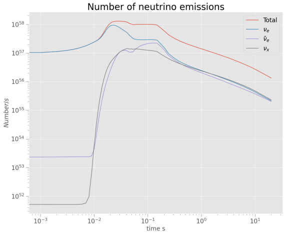

Figure 20: Number of Emissions from Nalazato Model 30$M_\odot$

CCSN Neutrino Flux Models

- **EOS** : **LS 220, SHEN, BH...**
- Metallicity: Solar (**Z=0.02**) and Small Magellanic Cloud SMC (**Z=0.004**)
- **Mass** range :**8-50** $M_{\odot}$
- Time burst duration:**0.5** to **20** s

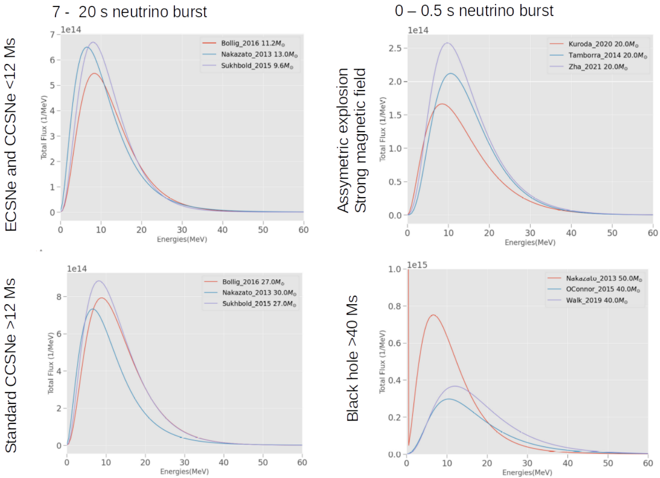

GEANT 4 IBD Spectrums

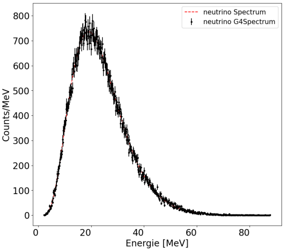

Figure 21: Simulate G4 Neutrino Spectrum at time 0.1s for Nakzato Model at 10 kpc

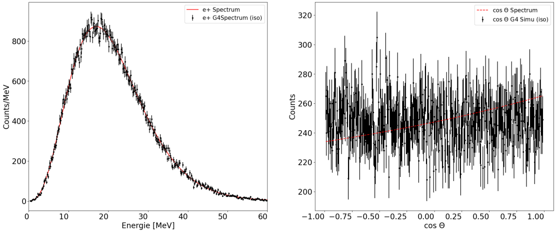

Figure 22: Simulate G4 Positron Energy and Angular Spectrum at time 0.1s for Nakzato Model at 10 kpc

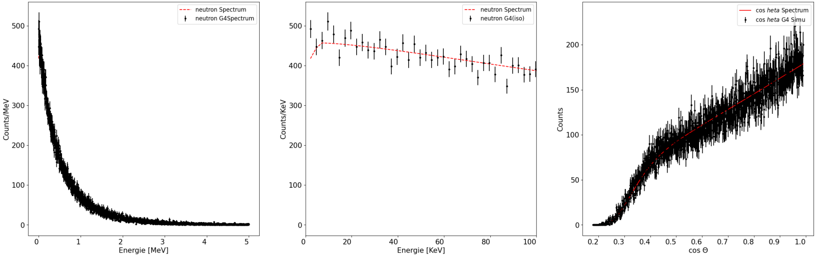

Figure 23: Simulate G4 Neutron Energy and Angular Spectrum at time 0.1s for Nakzato Model at 10 kpc

SN neutrino Electron Scattering

$$\frac{dN}{dtdE} = N_{H_2O} f_p \frac{1}{4\pi d^2} \frac{L(t)}{< E > (t)} \phi(E,t)\psi(t)\sigma(E) \qquad \sigma(E) = \int_{E_{e_1}}^{E_{e_2}} \frac{d\sigma(E, E_e)}{dE_e} dE_e \tag{9}$$

With f_p a factor related to layer external electrons in Water equal to 10.
The differential cross section takes into account the NC and CC. However, at SN neutrino energies only CC interaction is possible for the ν_e and $\bar{\nu}_e$.
The allowed values of E_e, $E_1 < E_e < E_2$, correspond to the possible scattering angles θ^{CM} in the center of mass (CM) frame:

$$E_e = m_E + \frac{(2m_E E_\nu^2 cos(\theta)^2)}{((m_E + E_\nu)^2 - E_\nu^2 cos(\theta)^2)} \tag{10}$$

$$E_1 = E_{ch} \qquad E_2 = mE + \frac{2E_\nu^2}{(2E_\nu + m_E)} \tag{11}$$

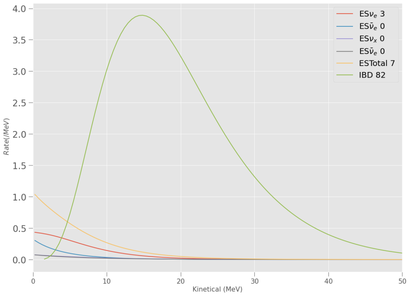

Figure 24: ES vs IBD Energy spectrum at 10 kpc for Nakazato model 30 $M_\odot$

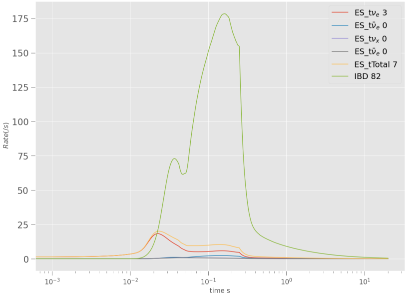

Figure 25: ES vs IBD Time spectrum at 10 kpc for Nakazato model 30 $M_\odot$

SN neutrino Electron Scattering Angular distribution

$$cos(\theta)) = \frac{(E_\nu + m_E)(E_e - m_e)}{E_\nu p_e} \quad (6)$$

The expression of $\frac{d\sigma(E, cos(\theta))}{dcos(\theta)}$ is obtained from $\frac{d\sigma(E, E_e)}{dE_e}$ [2]:

$$\frac{d\sigma(E, cos(\theta))}{dcos(\theta)} = \frac{d\sigma}{d\cos\theta}(E_\nu, \cos\theta) = \frac{dcos(\theta)}{dE_e}\frac{d\sigma}{dE_e} = \frac{4m_E E_\nu eNu(m_E + E_\nu)^2 cos(\theta)}{((m_E + E_\nu)^2 - E_\nu^2 cos(\theta)^2)^2}\frac{d\sigma}{dE_e} \quad (8)$$

- $N_{ES} \approx 10\% N_{IBD}$
  5-15 Events per burst at 10 kpc
- Directional information:
  Not enough rate at 10 kpc, but d¡5 kpc (20-60 events).
  Electron scattered contribution signal for kinetical energies T¿1 MeV far enough for the E_{th}.
- Discrimination between IBD and ES Cerenkov depositions.

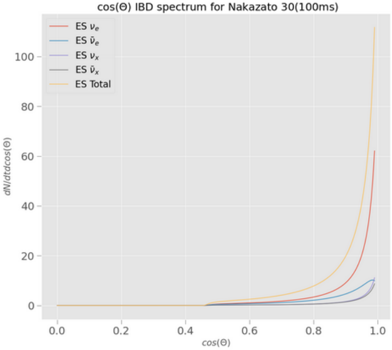

Figure 26: Spectrum for ES cosinus scattering angle, at time =0.1s for Nazazato model 30 $M_\odot$

SN Neutrino oscillations: neutrino propagation is described by 3 mass eigenstates: ν_1, ν_2, ν_3, with masses $m_1 < m_2 < m_3$ in Normal mass hierarchy.

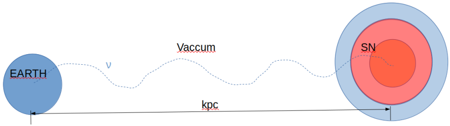

In vaccuum

The eigenvalues of each state $H_{0_i}\nu_i = E_i\nu_i$ with $E_i = \sqrt{p_i + m_i}$

The projection of each flavor β using the PMNS unitary matrix U [9] becomes:

$$\nu_\beta = \sum_{i=1,2,3} U_{\beta i}\nu_i \qquad \bar{\nu}_\beta = \sum_{i=1,2,3} U^*_{\beta i}\bar{\nu}_i \tag{12}$$

The transition probability between two states is:

$$P_{\alpha\rightarrow\beta} = |\nu_\alpha \nu_\beta|^2 = \delta_{\alpha\beta} - 4\sum_{j>k} Re\left\{U^*_{\alpha j}U_{\beta j}U_{\alpha k}U^*_{\beta k}\right\}\sin^2\left(\frac{\Delta_{jk}m^2 d}{4E}\right) +$$

$$2\sum_{j>k} Im\left\{U^*_{\alpha j}U_{\beta j}U_{\alpha k}U^*_{\beta k}\right\}\sin\left(\frac{\Delta_{jk}m^2 d}{2E}\right) \tag{13}$$

For example, parametrizing for two mixing angles $\bar{\theta}_{12}$, $\bar{\theta}_{13}$, we have for $\bar{e}$:

$$D_{\bar{e}1} = |U_{\bar{e}1}|^2 = cos^2\bar{\theta}_{12}cos^2\bar{\theta}_{13} \qquad D_{\bar{e}2} = |U_{\bar{e}2}|^2 = cos^2\bar{\theta}_{12}sin^2\bar{\theta}_{13} \qquad D_{\bar{e}3} = |U_{\bar{e}3}|^2 = sin^2\bar{\theta}_{13} \tag{14}$$

In matter

Hamiltonian becomes: $H_i = H_{O_i} + V_i$
Propagation eigenstates changes: $v_i \rightarrow v_{im}$ and $\theta_{ij} \rightarrow \theta_{ijm}$

$$\sin 2\bar{\theta}_{13m} = \frac{\sin 2\theta_{13}}{\sqrt{(\cos 2\theta_{13} + cos^2\theta_{12} V/k)^2 + \sin^2 2\theta_{13}}} \tag{15}$$

$$\cos 2\bar{\theta}_{13m} = \frac{\cos 2\theta_{13} + cos^2\theta_{12} V/k}{\sqrt{(\cos 2\theta_{13} + cos^2\theta_{12} V/k)^2 + \sin^2 2\theta_{13}}} \qquad k = \frac{\Delta m_{13}}{2E} \tag{16}$$

$$\sin 2\bar{\theta}_{12m} = \frac{\sin 2\theta_{12}}{\sqrt{(\cos 2\theta_{13} + V/k)^2 + \sin^2 2\theta_{12}}} \tag{17}$$

$$\cos 2\bar{\theta}_{12m} = \frac{\cos 2\theta_{12} + V/k}{\sqrt{(\cos 2\theta_{12} + V/k)^2 + \sin^2 2\theta_{12}}} \qquad k = \frac{\Delta m_{12}}{2E} \tag{18}$$

CC ($\nu_{e,\bar{e}} + e \rightarrow \nu_{e,\bar{e}} + e$) at SN energies lead to a difference of potential V:

$$\Delta V = V_e - V_x = \sqrt{2} G_F n_e \tag{19}$$

This add a resonance, depending on density n_e, with the condition [10]:

$$n_e^R = cos(2\theta_m) n_0 \qquad n_0 = \frac{\Delta m_{ij}^2}{2\sqrt{2} E G_F} \tag{20}$$

SN neutrino Transport effects: MSW Effect

SN environnemment:

The density variation, $n_e(t)$ leads to
H(t)= $H_0 + V(t)$
MSW effect : Adiabatic or partially adiabatic neutrino flavor conversion in medium with varying density [11].
Adiabaticity condition:

$$\gamma = \left| \frac{\dot{\theta}_m}{H_{im} - H_{jm}} \right| \ll 1 \qquad (21)$$

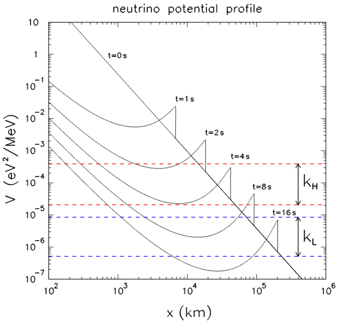

Figure 27: SN Neutrino potential profile [12]

At this point, several approximations can be done:

1)In high densites SN medium $\frac{V}{k} \gg 1$ and $cos2(\bar{\theta}_m) \approx 1$ $\quad sin2(\bar{\theta}_m) \approx 0$

2)The assumption of $N_\mu \equiv N_\tau = N_x$ leads to non observable effects of the transformation 2-3, i.e. $\theta_{23m} = 0$ in NMO. **3 flavor oscillation case with** θ_{12m} **and** θ_{13m}.

3) **In Vaccum** : $\bar{P}_{ex} \propto sin^2\Delta_{ij} = sin^2 \frac{\Delta m^2_{ij} d}{2E}$
At long distances 1 pc the factor $\frac{d}{E}$ averages out: $\bar{P}_{ex} \longrightarrow \langle \bar{P}_{ex} \rangle (\theta_{ij})$

Mean Probability will **only depend on** vaccum mixing angles θ_{ij}.

SN neutrino Transport effects: Observable spectrums

At **SN distances**(d≥1kpc) and neglecting **matter effects** in the SN core, oscillations probabilities depend only on the **mass ordering**:

For $\bar{\nu}_e$ in Normal mass ordering **NMO** [5]

$$\bar{p}_{ee} = D_{e1} = cos^2(\theta_{12})cos^2(\theta_{13}) \qquad \bar{p}_{ex} = 1 - \bar{p}_{ee} \qquad \bar{p}_{xx} = (1 + \bar{p}_{ee})/2 \qquad \bar{p}_{xe} = (1 - \bar{p}_{ee})/2 \tag{22}$$

For Inverted mass ordering **IMO** :

$$\bar{p}_{ee} = D_{e3} = sin^2(\theta_{13}) \qquad \bar{p}_{ex} = 1 - \bar{p}_{ee} \qquad \bar{p}_{xx} = (1 + \bar{p}_{ee})/2 \qquad \bar{p}_{xe} = (1 - \bar{p}_{ee})/2 \tag{23}$$

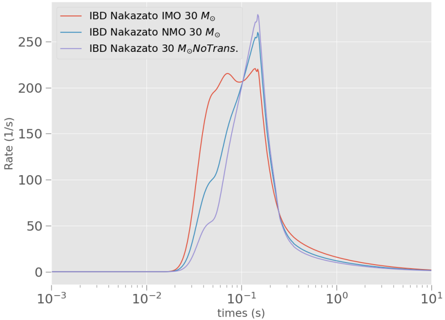

Figure 28: SN neutrino IBD rates including Non Adiabatic and Adiabatic MSW effect for NMO and IMO, at 10 kpc for Nakazato model 30 $M_\odot$

Earth spectrum becomes:

$$\frac{dN}{dEdt} = \bar{p}_{ee}\frac{dN}{dtdE}_{\bar{\nu}_e} + \bar{p}_{xe}\frac{dN}{dtdE}_{\bar{\nu}_x} \tag{24}$$

Values of mixing angles [13] $\theta_{12} = 33.44$ $\theta_{13} = 8.57$

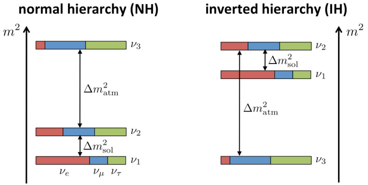

Figure 29: NMO and IMO neutrino mass eigenstates population

Diferential cross section

$$\frac{d\sigma(E, E_e)}{dE_e} = \frac{dt}{dE_e}\frac{d\sigma}{dt} \qquad t = m_n^2 + m_p - 2m_p(E_\nu - E_e) \qquad (25)$$

With $\frac{d\sigma}{dt}$ from [14]
Cherenkov light Threshold $E_{e_{th}} = \beta$ ¿ 1/n with n=1,333 = 0.7742 MeV
* For the neutrino $E_{ch} = 2.0684$ MeV

Limits of E_e, $E_1 < E_e < E_2$, correspond to the possible scattering angles θ^{CM} in the center of mass (CM) frame:

$$E_{1,2} = E_\nu - \delta - \frac{1}{m_p} E_\nu^{\mathrm{CM}} (E_e^{\mathrm{CM}} \pm p_e^{\mathrm{CM}}), \quad \text{with } \delta \equiv \frac{m_n^2 - m_p^2 - m_e^2}{2m_p} \qquad (26)$$

Positron Energy in the Lab frame

$$E_e = \frac{(E - \delta)(1 + \epsilon) + \epsilon cos(\Theta)\sqrt{((E - \delta)^2 - m_e^2 \kappa)}}{\kappa}$$

$$\epsilon = E/m_P \qquad \kappa = (1 + \epsilon)^2 - (\epsilon cos(\Theta))^2 \qquad (27)$$

Positron spectrum rate at a time t

$$\frac{dN}{dE_e dt}_{ibd}|_t = N_{H_2O} * f_p * \frac{1}{4\pi d^2} \int_{E_{min}}^{E_{max}} \frac{L(t)}{<E>(t)} \phi(E, t)\psi(t) \frac{d\sigma(E, E_e)}{dE_e} dE$$

$$\mathrm{E}_{min} = E_e + \delta \qquad E_{max} = \frac{E_{min}}{(1-2\frac{E_{min}}{m_p})} \qquad f_p = 2 \qquad (28)$$

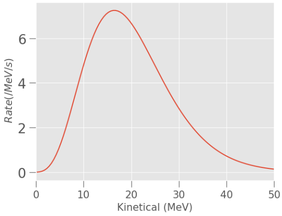

Figure 30: Positron spectrum at time 0.1 at the $\bar{\nu}_e$ peak production for Nakazato Model at 10 kpc

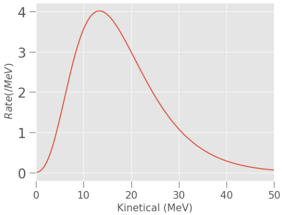

Figure 31: Total Positron spectrum for Nakazato Model at 10 kpc

IBD Positron Scattering angle distributions

Positron scattering angle in the Lab frame

$$cos(\theta) = \frac{(m_n^2 - m_p^2 - m_e^2 + 2m_p(E_\nu - E_e) - 2E_\nu E_e)}{2E_\nu p_e} \quad (29)$$

Diferential cross section

$$t = me^2 - 2E_\nu(E_e - p_e cos(\theta)) \quad (30)$$

Using the Jacobian transformation from $\frac{d\sigma}{dE_e}$ using the values of the implicits function of t and $cos(\theta)$:

$$\frac{\partial cos(\theta)}{\partial E_e} = \frac{1 + \epsilon(1 - \frac{E_e}{p_e} cos(\theta))}{\epsilon p_e} \quad (31)$$

$$\frac{d\sigma(E, cos(\theta))}{dcos(\theta)} = (\frac{\partial cos(\theta)}{\partial E_e})^{-1} \frac{d\sigma}{dE_e} = \frac{p_e \varepsilon}{1 + \varepsilon(1 - \frac{E_e}{p_e} \cos\theta)} \frac{d\sigma}{dE_e} \quad (32)$$

$cos(\theta)[-1, 1]$

$$\frac{dN}{dcos(\theta)dt}_{ibd}|_t = N_{H_2O} * f_p * \frac{1}{4\pi d^2} \int_E \frac{L(t)}{< E > (t)} \phi(E, t)\psi(t) \frac{d\sigma(E, cos(\theta))}{dcos(\theta)} dE \quad (17)$$

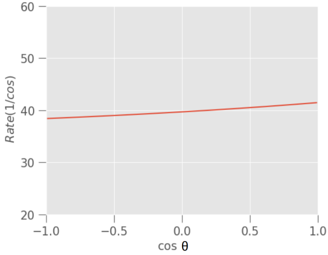

Figure 32: Scattering angle cosinus spectrum for Nakazato model at 10 kpc

At SN neutrinos energies, positron emission is barely **isotropic**.

IBD Neutron Energy distributions

Diferential cross section

$$\frac{d\sigma}{dE_n}(E_\nu, E_n) = \frac{\partial t}{\partial E_n}\frac{d\sigma}{dt} = -2m_p\frac{d\sigma}{dt} \tag{33}$$

Limits of E_n, $E_1 < E_n < E_2$ for an E_ν and E_e:

$$E_{n_{1,2}} = \frac{m_n^2 + m_p^2 - m_e^2 + 2E_\nu(E_e \mp p_e)}{2m_p} \tag{34}$$

Using the CM :

$$E_{n_{1,2}} = E_\nu - \Delta - \frac{E_{\nu CM}}{m_p}(E_{nCM} \mp p_{nCM}) \tag{23}$$

Neutron Energy in the Lab frame

$$E_n = \frac{-(1+\epsilon)(\Delta - E_\nu) + \epsilon cos(\theta_N)\sqrt{(\Delta - E_\nu)^2 - m_N^2\kappa}}{\kappa}$$

$$\Delta = \frac{-m_p^2 - m_n^2 + m_e^2}{2m_p} \tag{35}$$

Neutron Energy Spectrum at a given time

$$\frac{dN}{dE_e dt}_{ibd}|_t = N_{H_2O} f_p \frac{1}{4\pi d^2}\int_{E_{min}}^{E_{max}} \frac{L(t)}{<E>(t)}\phi(E,t)\psi(t)\frac{d\sigma(E,E_n)}{dE_n}dE$$

$$\text{E}_{min} = \frac{-2m_p(E_n+\Delta)}{(2(-p_n+E_n-m_p))} \qquad E_{max} = 100 \tag{36}$$

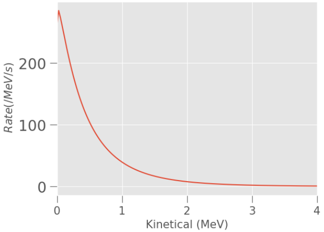

Figure 33: Neutron spectrum at time 0.1 at the $\bar{\nu}_e$ peak production for Nakazato Model at 10 kpc

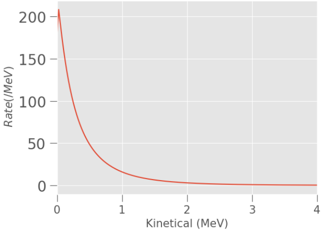

IBD Neutron Scattering angle distributions

Neutron scattering angle in the Lab frame

$$cos(\theta_N) = \frac{\Delta - (E_\nu - E_n) + \epsilon E_n}{\epsilon p_n} \quad (37)$$

The recoil of the neutron direction angle domain is bounded $M_N >> E_\nu$ in backwards angles, having a maximu apperture angle, related to $cos(\theta_{N_{max}})$

$$cos(\theta_{N_{max}}) = \frac{\sqrt{(2E_\nu \delta_S - (\delta_S^2 - m_e^2))}}{E_\nu} \qquad \delta_S = m_n - m_p \quad (38)$$

Differential cross section

$$\frac{\partial cos(\theta)}{\partial E_n} = -\frac{1 + \epsilon(1 - \frac{E_n}{p_n} cos(\theta_N))}{\epsilon p_N} \quad (39)$$

$$\frac{d\sigma(E_\nu, cos(\theta_N))}{dcos(\theta_N)} = (\frac{\partial cos(\theta)}{\partial E_n})^{-1} \frac{d\sigma}{dE_n} = -\frac{p_n \varepsilon}{1 + \varepsilon(1 - \frac{E_n}{p_n} \cos(\theta_N)} \frac{d\sigma}{dE_n} \quad (40)$$

We see that the distribution of the neutron scattering angle give us, some (poor) information about the arrive, that may be complemented with directional information of NC elastic scattering [15].

$$\frac{dN}{dcos(\theta)dt}_{ibd}|_t = N_{H_2O} f_p \frac{1}{4\pi d^2} \int_E \frac{L(t)}{< E > (t)} \phi(E,t)\psi(t) \frac{d\sigma(E, cos(\theta_N))}{dcos(\theta_N)} dE \quad (28)$$

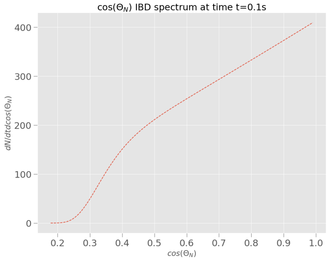

Figure 35: Neutrino cosinus scattering angle distribution

Back up PMNS Matrix

The standard parameterization of U_{PMNS} **PDG** is known to take the following form given by $U_{PMNS} = UK$ with

$$\begin{aligned} U &= \begin{pmatrix} c_{12}c_{13} & s_{12}c_{13} & s_{13}e^{-i\delta} \\ -c_{23}s_{12} - s_{23}c_{12}s_{13}e^{i\delta} & c_{23}c_{12} - s_{23}s_{12}s_{13}e^{i\delta} & s_{23}c_{13} \\ s_{23}s_{12} - c_{23}c_{12}s_{13}e^{i\delta} & -s_{23}c_{12} - c_{23}s_{12}s_{13}e^{i\delta} & c_{23}c_{13} \end{pmatrix}, \\ K &= \mathrm{diag}(1, e^{i\phi_2/2}, e^{i\phi_3/2}), \end{aligned} \tag{41}$$

where $c_{ij} = \cos\theta_{ij}$ and $s_{ij} = \sin\theta_{ij}$ and θ_{ij} represents a ν_i-ν_j mixing angle (i, j=1,2,3). Some experimental observation of three mixing angles are summarized as follows [16]:

$$\begin{aligned} \sin^2\theta_{12} &= 0.304^{+0.013}_{-0.012}\ (\mathrm{NH\ or\ IH}), \\ \sin^2\theta_{23} &= 0.452^{+0.052}_{-0.028}\ (\mathrm{NH}), 0.579^{+0.025}_{-0.037}\ (\mathrm{IH}), \\ \sin^2\theta_{13} &= 0.0218^{+0.0010}_{-0.0010}\ (\mathrm{NH}), 0.0219^{+0.0011}_{-0.0010}\ (\mathrm{IH}), \\ \delta(^\circ) &= 306^{+39}_{-70}\ (\mathrm{NH}),\quad 254^{+63}_{-62}\ (\mathrm{IH}), \end{aligned} \tag{42}$$

[1] J. F. Beacom, *The Diffuse Supernova Neutrino Background*. Ann.Rev.Nucl.Part.Sci.60:439-462, 2010. DOI: 10.1146/annurev.nucl.010909.083331.

[2] A. V. Filippenko, "Supernova 1987K: Type II in Youth, Type Ib in Old Age," *aj*, vol. 96, p. 1941, Dec. 1988. DOI: 10.1086/114940.

[3] R. F. Lang, C. McCabe, S. Reichard, M. Selvi, and I. Tamborra, "Supernova neutrino physics with xenon dark matter detectors: A timely perspective," *Physical Review D*, vol. 94, no. 10, Nov. 2016. DOI: 10.1103/physrevd.94.103009. [Online]. Available: https://doi.org/10.11032Fphysrevd.94.103009.

[4] A. Y. Smirnov, *The mikheyev-smirnov-wolfenstein (msw) effect*, 2019. DOI: 10.48550/ARXIV.1901.11473. [Online]. Available: https://arxiv.org/abs/1901.11473.

[5] A. L. Baxter, S. BenZvi, J. C. Jaimes, *et al.*, *Snewpy: A data pipeline from supernova simulations to neutrino signals*, 2021. DOI: 10.48550/ARXIV.2109.08188. [Online]. Available: https://arxiv.org/abs/2109.08188.

[6] A. Habig, "Snews – the supernova early warning system," *Nuclear Physics B - Proceedings Supplements*, vol. 143, p. 543, 2005, NEUTRINO 2004, ISSN: 0920-5632. DOI: https://doi.org/10.1016/j.nuclphysbps.2005.01.208. [Online]. Available: https://www.sciencedirect.com/science/article/pii/S0920563205002422.

[7] P. Bhattacharjee, A. Bandyopadhyay, S. Chakraborty, S. Ghosh, K. Kar, and S. Saha, *Inelastic charged current interaction of supernova neutrinos in two-phase liquid xenon dark matter detectors*, 2020. DOI: 10.48550/ARXIV.2012.13986. [Online]. Available: https://arxiv.org/abs/2012.13986.

[8] E. Baron, J. Cooperstein, and S. Kahana, "Type ii supernovae in $12\mathrm{M}_{\mathrm{cirdot}}$ and $15\mathrm{M}_{\mathrm{cirdot}}$ stars: The equation of state and general relativity," *Phys. Rev. Lett.*, vol. 55, pp. 126–129, 1 Jul. 1985. DOI: 10.1103/PhysRevLett.55.126. [Online]. Available: https://link.aps.org/doi/10.1103/PhysRevLett.55.126.

[9] J. Iizuka, T. Kitabayashi, Y. Minagawa, and M. Yasuè, "Parametrization of pontecorvo–maki–nakagawa–sakata mixing matrix based on CP-violating bipair neutrino mixing," *Modern Physics Letters A*, vol. 30, no. 05, p. 1 550 019, Feb. 2015. DOI: 10.1142/s0217732315500194. [Online]. Available: https://doi.org/10.1142%2Fs0217732315500194.

[10] A. Y. Smirnov, "The MSW effect and matter effects in neutrino oscillations," *Physica Scripta*, vol. T121, pp. 57–64, Jan. 2005. DOI: 10.1088/0031-8949/2005/t121/008. [Online]. Available: https://doi.org/10.1088%2F0031-8949%2F2005%2Ft121%2F008.

[11] K.-C. Lai, C. S. J. Leung, and G.-L. Lin, *Testing msw effect in supernova explosion with neutrino event rates*, 2020. DOI: 10.48550/ARXIV.2001.08543. [Online]. Available: https://arxiv.org/abs/2001.08543.

[12] G. L. Fogli, E. Lisi, A. Mirizzi, and D. Montanino, "Analysis of energy and time dependence of supernova shock effects on neutrino crossing probabilities," *Physical Review D*, vol. 68, no. 3, Aug. 2003. DOI: 10.1103/physrevd.68.033005. [Online]. Available: https://doi.org/10.1103%2Fphysrevd.68.033005.

[13] I. Esteban, M. Gonzalez-Garcia, M. Maltoni, T. Schwetz, and A. Zhou, "The fate of hints: Updated global analysis of three-flavor neutrino oscillations," *Journal of High Energy Physics*, vol. 2020, no. 9, Sep. 2020. DOI: 10.1007/jhep09(2020)178. [Online]. Available: https://doi.org/10.1007%2Fjhep09%282020%29178.

[14] A. Strumia and F. Vissani, "Precise quasielastic neutrino/nucleon cross-section," *Physics Letters B*, vol. 564, no. 1-2, pp. 42–54, Jul. 2003. DOI: 10.1016/s0370-2693(03)00616-6. [Online]. Available: https://doi.org/10.1016%2Fs0370-2693%2803%2900616-6.

[15] A. G. Rosso, F. Vissani, and M. C. Volpe, "What can we learn on supernova neutrino spectra with water cherenkov detectors?" *Journal of Cosmology and Astroparticle Physics*, vol. 2018, no. 04, p. 040, Apr. 2018. DOI: 10.1088/1475-7516/2018/04/040. [Online]. Available: https://dx.doi.org/10.1088/1475-7516/2018/04/040.

[16] M. C. Gonzalez-Garcia, M. Maltoni, and T. Schwetz, "Updated fit to three neutrino mixing: Status of leptonic CP violation," *Journal of High Energy Physics*, vol. 2014, no. 11, Nov. 2014. DOI: 10.1007/jhep11(2014)052. [Online]. Available: https://doi.org/10.1007%2Fjhep11%282014%29052.